IEEE
Advancing Technology for Humanity

IEEE UKRAINE SECTION

LVIV
OPEN TO THE WORLD

Lviv Convention Bureau

IEEE UKRCON-2021

2021 IEEE 3rd Ukraine Conference on Electrical and Computer Engineering

August 26 – 28, 2021, Lviv, Ukraine

Conference Proceedings

Track 1:
Microwave Techniques, Antennas & Radar Systems

Track 1:
Microwave Techniques, Antennas & Radar Systems
Special Session:
Adaptive Antenna Arrays and Smart Antennas

Track 1:
Microwave Techniques, Antennas & Radar Systems
Special Session:
UWB Signals, Signal Processing & Electromagnetic Compatibility

Track 3:
Industrial and Power Electronics & Energy Systems

Track 4:
Industry Applications, Automation & Industry 4.0

Track 5:
Nanotechnologies, Photonics, Electron Devices & Magnetics

Track 6:
Systems Analysis, Reliability, Computer Science & Communications

Track 7:
Engineering Education & History

Part Number: CFP21K03-USB
ISBN: 978-1-6654-0093-0

Copyright and Reprint Permission: Abstracting is permitted with credit to the source. Libraries are permitted to photocopy beyond the limit of U.S. copyright law for private use of patrons those articles in this volume that carry a code at the bottom of the first page, provided the per-copy fee indicated in the code is paid through Copyright Clearance Center, 222 Rosewood Drive, Danvers, MA 01923. For reprint or republication permission, email to IEEE Copyrights Manager at pubs-permissions@ieee.org. All rights reserved. Copyright ©2021 by IEEE.

Organizers and Partners

The IEEE UKRCON-2021 is organized by

IEEE Ukraine Section

Conference Partners:

IEEE Ukraine Section (West) AP/ED/MTT/CPMT/SSC Societies Joint Chapter

IEEE Ukraine Section (East) AP/MTT/ED/AES/GRS/NPS Societies Joint Chapter

IEEE Ukraine Section (Kyiv) ED/MTT/CPMT/COM/SSC Societies Joint Chapter

IEEE Ukraine Section (Rep of Georgia) ED/MTT Societies Joint Chapter

IEEE Ukraine Section CAS/IM/C/MTT Societies Joint Chapter

IEEE Ukraine Section PHO Society Chapter

IEEE Ukraine Section (Kharkiv) SP/AP/C/EMC/COM Societies Joint Chapter

IEEE Ukraine Section IM/CIS Societies Joint Chapter

IEEE Ukraine Section SP/AES Societies Joint Chapter

IEEE Ukraine Section EMB Society Chapter

IEEE Ukraine Section PE/IE/IA Societies Joint Chapter

Proceedings

Edited by Mariya Antyufeyeva

Computer layout and cover design: Mariya Antyufeyeva

2021 IEEE 3rd Ukraine Conference on Electrical and Computer Engineering (UKRCON)

IEEE Catalog Number: CFP21K03-USB

ISBN: 978-1-6654-0093-0

Copyright and Reprint Permission: Abstracting is permitted with credit to the source. Libraries are permitted to photocopy beyond the limit of U.S. copyright law for private use of patrons those articles in this volume that carry a code at the bottom of the first page, provided the per-copy fee indicated in the code is paid through Copyright Clearance Center, 222 Rosewood Drive, Danvers, MA 01923. For reprint or republication permission, email to IEEE Copyrights Manager at pubs-permissions@ieee.org. All rights reserved. Copyright ©2021 by IEEE.

Table of Contents

Technical Papers

Microstrip Antenna with Complex Topology Fed by Coplanar Line

Dmitriy V. Mayboroda
V. N. Karazin Kharkiv National University
Kharkiv, Ukraine
shfmayboroda@gmail.com

Sergey A. Pogarsky
V. N. Karazin Kharkiv National University
Kharkiv, Ukraine
spogarsky@gmail.com

David Korsakov
V. N. Karazin Kharkiv National University
Kharkiv, Ukraine
davidorina19@gmail.com

***Abstract*—The paper presents the results of numerical modeling of the spectral and energy characteristics of a microstrip antenna with slot inhomogeneities of complex topology. Simulation was carried out within the framework of a semi-open resonator model by the finite element method using the Ansoft HFSS software product. The influence of the geometric dimensions and material constants of the structure on the frequency and energy characteristics is investigated.**

Keywords—microstrip monopole, coplanar, pattern characteristic, matching

I. INTRODUCTION

The main trend in the development and creation of a new generation of the element base of functional elements of the microwave, K_a and terahertz ranges is the search for both new physical effects as a physical basis for the operation elements, and the search for new design solutions. The need for the development of the element base is due, first of all, to the solution of a lot of applied problems, including geolocation, the development of new methods of medical diagnostics (radiometry, radiotomography, radio-introscopy). Among the most promising new technical implementations, one can point to structures based on hybrid metal-dielectric structures (HMDS) of planar and volumetric shaping. The structures of this kind allow to realize the potential capabilities of radiating elements both in a single design and as part of antenna arrays [1, 2]. Realization of potential possibilities requires the solution of another important problem - the formation of the necessary distribution of electromagnetic fields in a given space to create conditions for the effective interaction of fields with existing inhomogeneities, for example, with slot inhomogeneities of various topologies for effective radiation and the creation of the necessary polarization and spatial-energy characteristics.

If we assess the prospects of using certain design solutions based on the results of scientific and technical conferences and publications in specialized publications, then it can be argued that radiating systems implemented using technologies of film hybrid integrated circuits in the microwave range are the most preferable [3]. Technical solutions based on planar HMDS have undeniable advantages. The main of which is low profile (including conformity) [4]. The second advantage is the possibility of realizing practically any topological configuration of radiating and auxiliary elements on a dielectric substrate, which allows realizing practically any functional elements [5, 6]. Of course, the indisputable advantages include compactness, light weight, high reproducibility of parameters and low production costs.

At the same time, the classical design of a planar HMDS presupposes the presence of the main structural elements: a dielectric substrate, one side of which, as a rule, is metallized, and on the other side, there are conductors with different topologies that perform certain functional actions and elements of the excitation system. By itself, such a design, a priori, has significant drawbacks. The main one is that the volume within which the energy is stored turns out to be insufficiently large (a thin plate compared to the wavelength), and, consequently, the quality factor of such systems is low. The second is a narrow band, which is associated, among other things, with the possibility of multiple resonances, and with the possibility of exciting surface waves in the substrate. Another essential aspect is the method of excitation of the structure: either using direct galvanic contact of functional elements with external exciting circuits, or using a conductive excitation method, or using slot exciters. All these methods to a greater or lesser extent narrow the working range of the structure.

This paper presents the results of modeling the main characteristics of a structure representing a microstrip resonator with inhomogeneities in the form of slotted discs with slits. A distinctive feature of the structure is the absence of a ground plane. The excitation of the structure is carried out using a segment of a coplanar line.

II. STRUCTURE UNDER STUDY

An isometric view and topology of conductors with a notation system are shown in Fig. 1. The topology of inhomogeneities has a complex structure: disc slot inhomogeneities are combined with segments of slot inhomogeneities of the linear type (slits). In Fig. 1, the following designations are used: 1 - basic disc resonator, dielectric substrate, 2 - dielectric substrate, 3 - slot-type inhomogeneities. The use of a complex topology of slot inhomogeneities is due to the need to solve two key problems. The first of them is associated with the need to reduce the number of degenerate eigenmodes in the working band. As it is known [7], in the spectrum of eigenmodes of electrodynamic structures with axial symmetry, there was a countable set of degenerate eigenmodes. This property significantly reduces the level of electrodynamic characteristics due to the instability of the wave regime near frequencies where degenerate eigenmodes can be excited.

The second is associated with the need to shift the operating range to a lower frequency region while maintaining the specified geometric dimensions by increasing the length of the radiating aperture, which is

978-1-6654-0093-0/21/$31.00 ©2021 IEEE

achieved by increasing the length of the current lines flowing over the disc surface.

The structure is excited using a segment of an unshielded coplanar line (there is no metallization on the back side of the substrate).

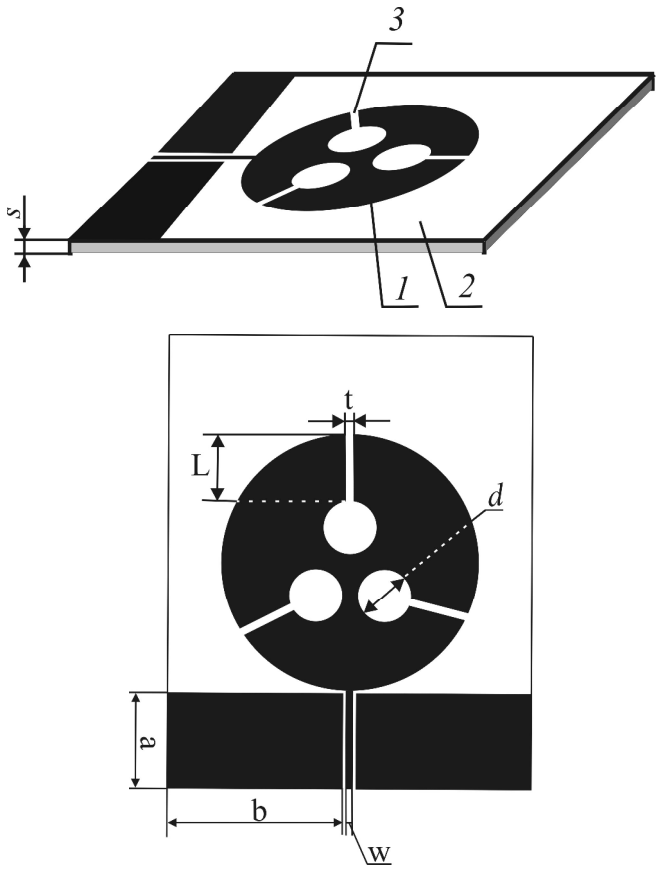

Fig. 1. Schematic sketch of the structure.

Based on the assumption that the structure operates in the microwave range, the following parameters were chosen: the diameter of the microstrip disc is 35 mm, the thickness of the dielectric substrate is 0.5 mm, the length of the linear part of the inhomogeneity is variable and depends on the diameter of the axial inhomogeneity (initial value $L = 6$ mm, final value $L = 4$ mm), diameter of the axial heterogeneity - variable (change interval is 6, 8, 10 mm), the gap width of the linear part of the heterogeneity is fixed and equal to $t = 1$ mm. The values of the relative permittivity of the substrate were selected from a number of standard values ($\varepsilon_r = 2.2, 2.4, 3.8$). As a basic method for the analysis of spectral and energy characteristics, the finite element method was used, which is numerically implemented using the Ansoft HFSS package [8].

III. Results of The Study

In the numerical simulation of the characteristics of the structure under consideration, the method of a half-open resonator was used [9]. In this case, the condition $s < \lambda_r$ is assumed to be fulfilled. Due to the absence of a shielding plane, the nature of the distribution of currents on the surface of the resonator and electromagnetic fields both in the dielectric substrate and in the near zones above the microstrip resonator and on the opposite side of the substrate changes fundamentally. It is quite obvious that the field distribution is frequency dependent. Information about possible resonances of eigenwaves in the structure can be obtained from the spectral characteristics.

A. Eigenmodes Spectrum

It is known that the spectral characteristic is a key element in the study of complex compositional electrodynamic structures. It gives an idea not only of the number of eigenresonance frequencies in the frequency range under consideration and their distribution on the frequency axis, which makes it possible to estimate the operating range of the structure, but also to evaluate the possibility of the occurrence of modes with frequency and polarization instability due to the existence of degenerate modes of oscillations. In Fig. 2 the spectral characteristic of the structure with the following set of parameters: $d = 6$ mm, $\varepsilon_r = 2.4$, $s = 0.5$ mm is shown.

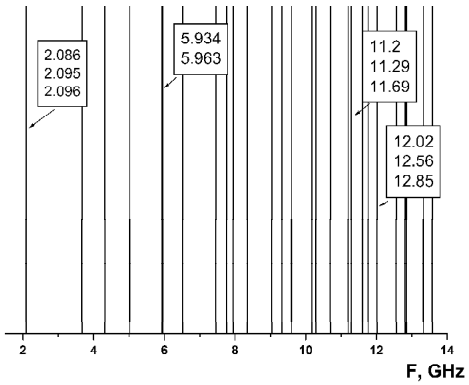

Fig. 2. The eigenmode spectrum of structure under study.

The analysis of the spectral characteristics indicates a significant non-uniformity of the distribution of spectral lines on the frequency axis. Moreover, in the low-frequency region (up to approximately 10 GHz), the spectrum turns out to be rather sparse. In the high-frequency part of the range (10 ... 14 GHz), the spectrum is noticeably denser, but it remains significantly uneven. Comparison of this characteristic with the characteristic given in [10], in which the structure excited by a segment of a microstrip line was considered, shows that, upon excitation by a segment of a coplanar line, the spectrum of eigenmodes turns out to be significantly "poor". The physical explanation of this fact is that in the absence of a screening plane, the conditions for the excitation of a part of eigenmodes disappear. Near a frequency of 2 GHz, there is practically a degeneration of three types of modes, the resonance frequencies of which differ by no more than 10 MHz. Near the 6 GHz frequency, the spectral lines of the two eigenmodes of oscillations approach quite closely (the frequency difference is 29 MHz). In this situation, we can speak of a situation with a potential "technical" possibility of degeneration (due to the instability of the operation of the exciting generator). In the high-frequency part of the frequency range under consideration, there is no degeneration of eigenmodes (the difference between the resonant frequencies of eigenmodes is at least 300 MHz). Thus, it is possible to predict the existence of stable modes of operation in the high-frequency

region near frequencies of 11 GHz and 12 GHz. At the same time, near these frequencies, it is possible to implement tunable controlled devices.

B. Matching

The question of optimal matching of any functional element with the exciting circuits is the key both in the microwave range and in higher wavelength ranges. The efficiency directly depends on the degree of matching functional element, in addition, the design features of the matching element can affect the spectral characteristics due to the fact that unwanted resonances can occur in these elements. By itself, the structure under consideration is a complex composition: a disc resonator, slot inhomogeneities of the disc type, slot inhomogeneities of the linear type, and, finally, a segment of the coplanar line acting as an exciter, each of which has a certain set of eigenresonance frequencies. The interaction of all these elements leads to the resulting spectral, amplitude-frequency and energy characteristics. Two main factors have a significant effect on the $|S_{11}|$ characteristic indicating the degree of matching: the dielectric substrate (more precisely, the value of the relative permittivity of the substrate) and the topological features of the slot disc inhomogeneities (the diameter of the discs and parameters of slits).

In Fig. 3 the frequency dependences of $|S_{11}|$ for a fixed value of the diameter of the slot disc resonator $d = 8$ mm at relatively small values of ε_r are shown. The choice of ε_r values is dictated by two circumstances: first, at small values, the amplitude of (possible!) surface waves turns out to be lower; second, at small values of ε_r, the effect of redistribution of the energy of excited oscillations in the regions above and below the microstrip disc is less pronounced.

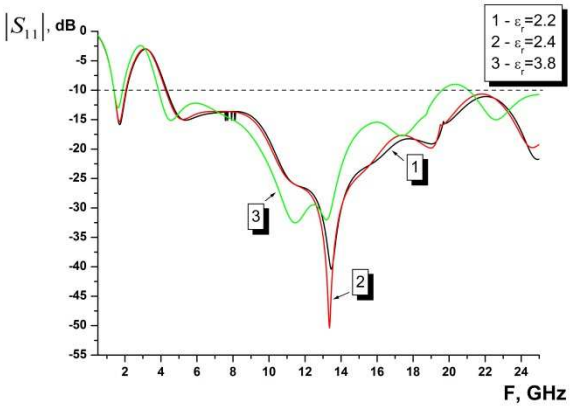

Fig. 3. The dependences of $|S_{11}|$ vs frequency with ε_r variation.

Obviously, in the frequency range from 4 GHz to 22 GHz with the selected values of ε_r, the level of return loss $|S_{11}|$ does not exceed -10 dB. In this case, a smoother character of the dependence is observed at $\varepsilon_r = 3.8$. At lower values of ε_r, although a lower level of -50 dB is attainable in the peaks, in general the curves are oscillatory.

The diameter of the disc slot inhomogeneities has a significant effect on the degree of matching with external circuits. In Fig. 4 the dependences of $|S_{11}|$ in the frequency band with variation of the diameter of the disc inhomogeneities are shown.

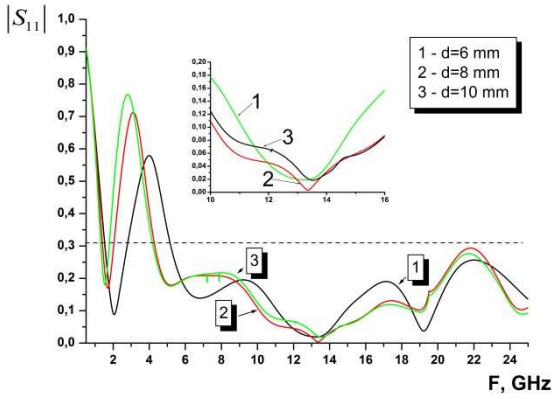

Fig. 4. The dependences of $|S_{11}|$ vs frequency with d variation.

The analysis of the dependences shows that, regardless of the diameter of the inhomogeneities in the frequency band from 5 GHz to 24 GHz, it is possible to achieve the optimal matching level (the dashed line corresponds to the VSWR = 2). Moreover, at the optimal value of the diameter $d = 8$ mm (curve 2) in the frequency range from 10 to 14.5 GHz, the values of $|S_{11}|$ do not exceed 0.1 (which is equivalent to VSWR <1.2).

C. Radiation Pattern

The ability to create a certain spatial distribution of fields is determined by the type of radiation pattern. In Fig. 5 the radiation patterns in the elevation plane (θ plane) with variations in values at a fixed frequency of $F = 12.56$ GHz and $d = 10$ mm are shown. The angle θ was measured from the normal to the antenna plane at a fixed angle $\varphi = 90^0$. All charts are normalized to the global maximum recorded for the value of $\varepsilon_r = 3.8$. Dependency analysis shows that for all values of ε_r the diagrams are multi-lobed.

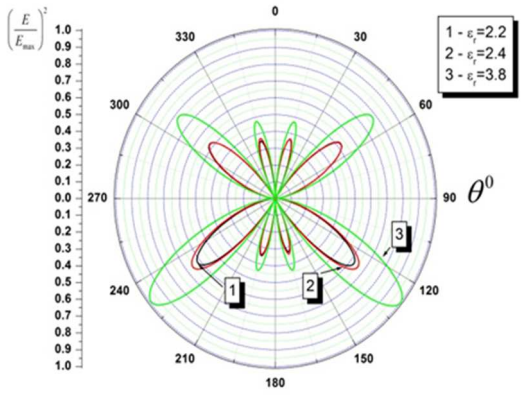

Fig. 5. Radiation patterns with variation of ε_r value.

Moreover, with an increase in the value of ε_r, the amplitude of the radiated signal increases. In this case, the amplitude of the radiated fields on both sides of the antenna

for small values is approximately the same. With an increase to 3.8, the amplitude of the radiated fields from the side of the dielectric substrate turns out to be much larger. The width of the petals weakly depends on the value at small values of ε_r.

With an increase of ε_r to 3.8, the width of the petals with a larger amplitude expands noticeably. In Fig. 6 the radiation patterns in the azimuthal plane (φ plane) with variations in values of ε_r at a fixed frequency of $F = 12.56$ GHz and a value of $d = 10$ mm are shown. The angle φ was measured from the axis of the central conductor of the coplanar line clockwise at a fixed value of $\theta = 0^0$. All dependences are normalized to the global maximum at $\varepsilon_r = 3.8$. Obviously, the diagrams at small values of ε_r turn out to be four-lobed.

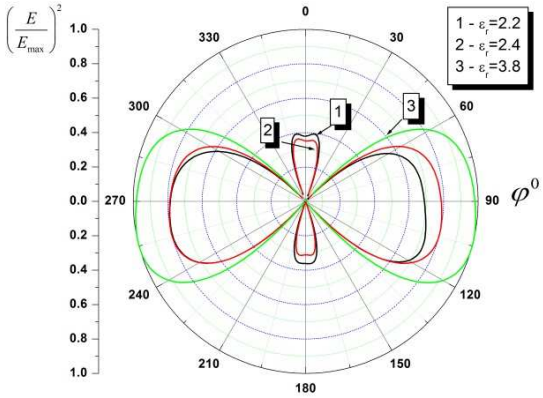

Fig. 6. Radiation patterns with variation of ε_r value.

As the value ε_r increases to 3.8, two lobes with relatively small amplitudes disappear. In this case, the width of the petals with large values of the amplitudes noticeably expands. The shape of the diagram is slightly asymmetrical about the selected directions 90^0 and 270^0.

Another important parameter that has a significant effect on both the shape of the radiation pattern and the level of the radiated power is the diameter of the slot inhomogeneities. The peculiarities of the influence of the diameter of the inhomogeneity can be traced from the changes in the shape of the diagram with the variation of the diameter by the example of the diagram in the azimuthal plane, which is shown in Fig. 7.

Comparison of the diagrams shown in Fig. 6 and Fig. 7 shows that at $\varepsilon_r = 2.4$ and the value of $d = 10$ mm the shape of the diagram practically does not change. At a relatively small value of the diameter $d = 6$ mm, a rotation of the direction of the radiation maximum by 90^0 is observed.

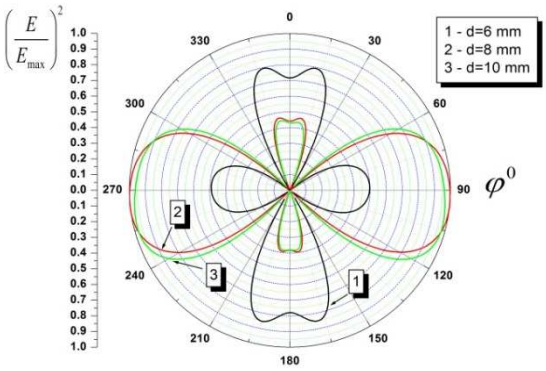

Fig. 7. Radiation patterns with variation of d value.

IV. Conclusions

The results of numerical simulation of the characteristics of a microstrip antenna with a complex topology of slot inhomogeneities when using a coplanar line segment as an exciter have shown the possibility of operating in a sufficiently wide frequency band. The nature of the influence of the geometric dimensions of the structural elements and the material parameters of the substrate on the spectral and energy characteristics of the antenna has been established. It can be predicted that, on the basis of such radiating structures, it is possible to create effective radiating systems (including as part of antenna arrays).

Acknowledgment

This work was supported by the Ministry of Education and Science of Ukraine, grant 0119U002535.

References

[1] T. Yoneyama, and S. Nishida, “Nonradiative dielectric waveguide circuit components”, Int. Jour. of Infrared and Millimeter Waves, Vol. 4, № 3, p. 439–449, 1983

[2] K. K. Singh, S.C.Gupta, “Review and Analysis of Microstrip Patch Array. Antenna with different configurations”, Int. J. of Scientific & Eng. Research, Volume 4, Issue 2, February 2013.

[3] 3. Z.Nei, W.C.Chew and Y.T.Lo, "Analysis of the annular-ring-loaded circular-disk microstrip antenna", IEEE Trans. Antennas Propag., vol. AP-38, No. 6, pp.806-813, June 1990.

[4] Juhua Liu, Quan Xue, Hang Wong at all. “Design and analysis of a low-profile and broadband microstrip monopolar patch antenna.” *IEEE Trans. Antennas Propag.*, Vol. 61, No. 01, pp.11-18, Jan 2013.

[5] D.V. Maiboroda and S.A.Pogarsky, "On the choice of optimal topology of a reflecting module based upon the circular-disk microstrip structure", J. Telecommunications and Radio Eng., vol.73, No.19,1713-1726, 2014.

[6] D.V.Maiboroda, and S.A.Pogarsky, “Electrodynamic Characteristics of the Disc Microstrip Radiators With Structural Auxiliary Elements”, J. Telecommunications and Radio Eng., Vol. 74, No. 13, pp.1147-1155, 2015.

[7] R.A Silin and V.P. Sazonov, Slow-wave structures, Moscow:Sov. Radio, 1966, 632 p. (in Russian).

[8] Ansoft HFSS /ANSYS Academic Research HF (5 tasks): 1 task(s) Permanent with TECS expiring 01-May-2020 Customer # 1076710.

[9] Kumar G., and Ray K.P. “Broadband microstrip antennas”, New York: Artech House, 2003.

[10] S. A. Pogarsky, L. N. Lytvynenko, and D. V. Mayboroda, “Design and Analysis of Microstrip Antenna with Disk Slot Discontinuities”, J. Telecommunications and Radio Eng., 78(19):1709-1718, 2019.

Operator Method in Approximate Solution of Dielectric Waveguide Eigenwaves Scattering by Graphene Strips

Mstislav E. Kaliberda
School of Radiophysics, Biomedical Electronics and Computer Systems
V.N. Karazin Kharkiv National University
Kharkiv, Ukraine
KaliberdaME@gmail.com

Sergey A. Pogarsky
School of Radiophysics, Biomedical Electronics and Computer Systems
V. Karazin Kharkiv National University
Kharkiv, Ukraine
Sergey.A.Pogarsky@univer.kharkov.ua

Lubov M. Kaliberda
Department of Physics
Kharkiv Petro Vasylenko National Technical University of Agriculture,
Kharkiv, Ukraine,
KaliberdaLM@gmail.com

***Abstract*—Approximate solution of a dielectric waveguide eigenwaves scattering by finite and semi-infinite system of graphene strips is presented. The operator method is used. We suppose that only waveguide eigenwaves can exist in the domain between the strips. Under this approximation integral operator equations become matrix ones. Their solution requires much less computation time. The solution of the co-called key problem, the scattering problem by a single graphene strip inside a dielectric slab, is obtained by the method of singular integral equations. The frequency dependences of scattering characteristics as well as radiation patterns are presented.**

Keywords—graphene, strip grating, operator equations, scattering, semi-infinite structure

I. Introduction

Scattering by strip gratings is a canonical problem. Strip grating with the dielectric slab can be used as antennas, absorbers, filters, etc. [1-3]. Graphene is a rather new 2D material. Its conductivity can be varied by application of external electrostatic or magnetostatic field, what opens great perspectives in creation of tunable devices [4, 5].

Finite-difference method is a widely used approach to graphene structures [6]. However, its accuracy is limited to several digits, since, for example, it uses the approximate radiation conditions. Another alternative is rigorous techniques such as method of integral equations or operator method, which allow to obtain results with required error at lower computation costs [7-9].

In [10], the non-linear operator equation relatively reflection operator of the semi-infinite system is obtained for the case if the scattered fields can be represented as Fourier series (discrete spectrum). In [11], the approach is extended to the semi-infinite gratings where scattered fields are represented as Fourier integrals (continuous spectrum). In [12], the operator method is used to scattering by finite and semi-infinite system of slots in the wall of a plane waveguide.

At the same time, approximate techniques require much less computation time [8]. In the case if the physical phenomena can be studied with limited accuracy, the approximate techniques are an adequate choice.

In this paper we consider scattering of the eigenwaves of the dielectric waveguide by finite and semi-infinite system of graphene strips inside the dielectric slab (see Fig.1). When we use the operator method, we divide solution of scattering problem into several steps. In such a way, we decrease the dimension of the resulting matrix equation. Operator method allows to obtain rigorous solution of the scattering problems. In the case if the scattered fields have continuous space spectrum (i.e. can be represented as Fourier integrals), the operator equations are integral ones. However if we suppose that only waveguide eigenwaves can propagate in the domain between the strips and the field scattered by one strip does not affect the other strips via free space, operator equations become matrix ones.

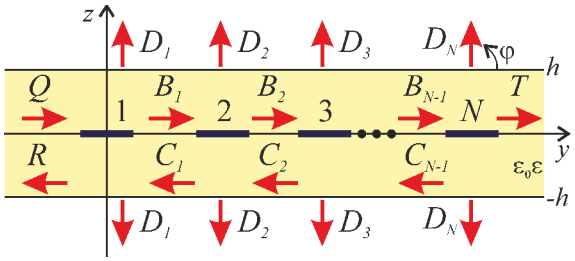

Fig. 1. Structure geometry.

Operator equations presented in this paper use scattering operators of a single strip. Thus at first we briefly present algorithm of obtaining of the reflection and transmission operators of a single strip which is based on the method of singular integral equations. After that, we write operator equations for finite and semi-infinite system of graphene strips.

II. Operators of a Single Graphene Strip

Suppose that the H -polarized p th eigenwave of the dielectric waveguide with amplitude q is incident from the domain $y<0$ on a single graphene strip which center coincides with the x -axis. The incident field we denote as qH^p, where H^p is known x -component of the magnetic field vector of the p th eigenwave with unit amplitude.

For graphene strip we use the following boundary conditions

$$\frac{1}{2}\left(E_y^+ + E_y^-\right) = \frac{1}{\sigma}\left(H_x^+ - H_x^-\right),\ z=0, \qquad (1)$$

$$E_y^+ = E_y^-,\ z=0, \qquad (2)$$

978-1-6654-0093-0/21/$31.00 ©2021 IEEE

where signs " $\pm$ " mean the limit value, if $z \to \pm 0$, σ is conductivity of graphene. It can be obtained from the Kubo formalism [4]. At the vacuum-dielectric interfaces we use the continuity conditions of the tangential components of the electric and magnetic field vectors as well as the radiation conditions at the infinity and the edge condition. The algorithm of reduction of the boundary-value problem for Helmholtz equation to the singular equation is presented in [13] in full details. Thus here we show only final results.

We introduce Fourier amplitude of the scattered field $b(\xi)$ with the help of the Fourier transform and the currents density on the strips

$$H_x^+(y,0) - H_x^-(y,0) = 2\int_{-\infty}^{+\infty} b(\xi)\exp(ik_1\xi y)d\xi, \qquad (3)$$

where $k_1 = k\sqrt{\varepsilon}$ is the wavenumber in the dielectric slab, $k = \omega\sqrt{\varepsilon_0\mu_0}$ is the wavenumber in vacuum. If function $b(\xi)$ is known than we can express field inside the slab, $|z| < h$ and above (below) the dielectric slab in the domain $|z| > h$. Scattered field inside the slab far from the strips can be represented as a sum of the eigenwaves of the dielectric waveguide, and field outside the slab can be represented as Fourier integral:

$$H(y,z) = \sum_{l=1}^{\infty} C_l b(\pm\beta_l)\sin(k_1 z\sqrt{1-\beta_l^2/\varepsilon}) \times \exp(\pm ik\beta_l y), \ if \ \ y \to \pm\infty, \ |z| < h, \qquad (4)$$

$$H(y,z) = \int_{-\infty}^{\infty} A(\xi)\exp(ik\xi y \pm ik\sqrt{1-\xi^2}z)d\xi, \ if \ |z| > h, \qquad (5)$$

where C_l are known constants which connect $b(\pm\beta_l)$ with the amplitudes of the eigenwaves of the dielectric waveguide, $A(\xi)$ is Fourier amplitude of the field above (below) the dielectric slab in the domain $|z| > h$. It can be expressed in terms of $b(\xi)$ [13].

We introduce function $F(y)$ which is the derivative of the currents density on the strips (up to the constant factor). Then

$$b(\xi) = \frac{1}{2\pi i\xi}\int_{-d}^{d} F(y)\exp(-ik_1 y\xi)dy. \qquad (6)$$

We can write (6) in the operator form:

$$b = \Xi\Im^{-1}F, \qquad (7)$$

where $\Im^{-1}$ is the inverse Fourier transform, operator Ξ acts as follow: $(\Xi g)(\xi) = g(\xi)/(i\xi)$, where $g(\xi)$ is an arbitrary function.

Unknown Fourier amplitude $b(\xi)$ can be obtained from the following singular integral equation, which we write in the operator form

$$b = \Xi\Im^{-1}(S+K)^{-1}E^p q \qquad (8)$$

where $E^p(y) = (\partial/\partial z)H^p(z=0)$, S is the singular operator and K is regular operator which act as follows:

$$(Sg)(y) = \frac{1}{\pi}PV\int_{-d}^{d}\frac{g(\xi)}{\xi - y}d\xi, \qquad (9)$$

$$(Kg)(y) = \frac{k_1}{\pi}\int_{-d}^{d}\left(\int_0^{\infty}\Gamma(\psi)\sin(k_1\xi(y-\xi))d\psi + \frac{1}{\pi}Z(y,\xi)\right)g(\xi)d\xi, \qquad (10)$$

$$Z(y,\xi) = \begin{cases} 2ik\pi(\sigma Z_0)^{-1}, \ if \ \ \xi \le y, \\ 0, \ if \ \ \xi > y, \end{cases} \qquad (11)$$

with condition $\int_{-d}^{d} g(\xi)d\xi = 0$, PV means Cauchy principal value integral, $Z_0 = 120\pi$ Ohm.

Function $\Gamma(\psi)$ satisfies the following asymptotic relation, $\Gamma(\psi) = 1/\psi^2 + O(1/\psi^4)$, if $\psi \to \infty$. The eigenwaves of the dielectric waveguide can be excited inside the slab. From the radiation conditions it follows that $\Gamma(\psi)$ has poles at the points which corresponds to the propagation constants β_l of these eigenwaves, $\Gamma(\psi) \sim 1/(\psi - \beta_l)$, if $\psi \to \beta_l$. Real values correspond to the propagating eigenwaves. To eliminate the singularities the regularization procedure is needed.

With the use of (8) we can introduce matrix reflection $r = (\mathrm{r}_{l,p})_{l,p=1}^{\infty}$ and transmission $t = (\mathrm{t}_{l,p})_{l,p=1}^{\infty}$ operators and radiation operator Ω of a single graphene strip, where

$$\mathrm{r}_{l,p} = C_l b(-\beta_l), \qquad (12)$$

$$\mathrm{t}_{l,p} = \delta_{l,p} + C_l b(\beta_l), \qquad (13)$$

$\delta_{l,p}$ is the Kronecker delta. Operator $\Omega = (\mathrm{a}_p)_{p=1}^{\infty}$ is vector which defines the far-field with elements

$$a_p(\xi) = A(\xi)\sqrt{1-\xi^2}. \qquad (14)$$

Eq. (14) is (up to the phase factor) the far-field representation of (5), $\xi = \cos\varphi$, φ is polar angle (see Fig.1).

III. Finite System of Strips

Let us consider the system of N graphene strips inside the dielectric slab. We suppose that eigenwaves of the dielectric waveguide are incident from the domain $y < 0$ (see Fig.1). The amplitudes of the incident waves are defined by the vector

Q. Suppose that reflection r_n, transmission t_n and radiation Ω_n operators of a single n th strip are known.

Let us denote the vector of the amplitudes of the eigenwaves of the dielectric waveguide which propagate in the positive and negative directions of the y-axis between the n th and $(n+1)$ th strip as B_n and C_n. The vector of the amplitudes of the reflected field we denote as R_N, the vector of the amplitudes of the transmitted field we denote as T_N. The Fourier amplitude of the field radiated by the n th strip of the system of strips we denote as D_n. The Fourier amplitude of the total radiated field we denote as D. They are connected by the following operator equations:

$$R_N = r_1 Q + t_1 e_1 C_1, \tag{15}$$

$$T_N = t_N e_{N-1} B_{N-1}, \tag{16}$$

$$B_1 = t_1 Q + r_1 e_1 C_1, \tag{17}$$

$$C_{N-1} = r_N e_{N-1} B_{N-1}, \tag{18}$$

$$B_n = t_n e_{n-1} B_{n-1} + r_n e_n C_n, \tag{19}$$

$$C_{n-1} = r_n e_{n-1} B_{n-1} + t_n e_n C_n, \ n = 2, 3, ..., N-1, \tag{20}$$

$$D_1 = \Omega_1 Q + \widetilde{\Omega}_1 e_1 C_1, \tag{21}$$

$$D_n = E_{n-1}^{-1}\left(\Omega_n e_{n-1} B_{n-1} + \widetilde{\Omega}_n e_n C_n\right), \tag{22}$$

$$D_N = E_{n-1}^{-1} \Omega_N e_{N-1} B_{N-1}, \tag{23}$$

$$D = \sum_{n=1}^{N} D_n. \tag{24}$$

The phase variation of the waves between the origin $y = 0$ and center of the $(n+1)$ th strip inside the dielectric waveguide is described by the operator e_n, and outside the waveguide is described by the operator E_n. Operator $\widetilde{\Omega}_n = (\widetilde{a}_{p,n})_{p=1}^{\infty}$ has elements $\widetilde{a}_{p,n}(\xi) = a_{p,n}(-\xi)$ and describes radiation if the eigenwaves are incident from the domain $y > 0$, where $a_{p,n}(-\xi)$ are elements of Ω_n.

IV. Semi-Infinite System of Strips

Let us consider semi-infinite periodic system of strips. Reflection operator R_∞ can be obtained from the non-linear operator equation [10]

$$R_\infty = r_1 + t_1 (I - e_1 R_\infty e_1 t_1)^{-1} e_1 R_\infty e_1 t_1, \tag{25}$$

where I is the unit operator.

Radiation operator Ω can be obtained with the use of the specific translation symmetry of the structure that means that no semi-infinite structure properties change with its last element removed. We can write two equations which connect the radiation operator of the semi-infinite structure and the Fourier amplitude of the radiated field D_∞:

$$D_\infty = \Omega Q, \tag{26}$$

$$D_\infty = \Omega_1 Q + \widetilde{\Omega}_1 e_1 C_1 + \Omega e_1 B_1. \tag{27}$$

After substitution (25) into (26) and after transformations obtain:

$$\Omega = \left(\Omega_1 + \widetilde{\Omega}_1 e_1 c_1\right)(I - e_1 b_1)^{-1}, \tag{28}$$

where operators c_1 and b_1 are

$$c_1 = R_\infty e_1 b_1, \tag{29}$$

$$b_1 = (I - r_1 e_1 c_1 R_\infty e_1)^{-1} t_1. \tag{30}$$

V. Numerical Results

With the use of (15)-(30) we study scattering and absorption characteristics of the finite and semi-infinite system of graphene strips.

Suppose that the first eigenwave of dielectric waveguide with symmetric distribution of the electric field with unit amplitude is incident on the periodic system of graphene strips. The period is $l = 70\mu m$. We consider graphene strips with electron relaxation time $\tau = 1$ ps and under room temperature $T = 300$ K. The chemical potential we denote as μ_c. The strip width is $2d = 20\mu m$. The width of the dielectric slab is $2h = 120\mu m$ and relative permittivity $\varepsilon = 2.25$.

Fig.2 shows dependences of the reflection R, transmission T, absorption A, and radiation Rad coefficients (power) on the frequency, $R + T + A + Rad = 1$.

Graphene strips can support plasmon resonances at THz. The maximum of radiation is observed near the first plasmon resonance frequency. However, the growth of absorption also takes place near the plasmon resonances what limits the radiation efficiency. For comparison, we also present results obtained by the method of singular integral equations (SIE). Good agreement is observed.

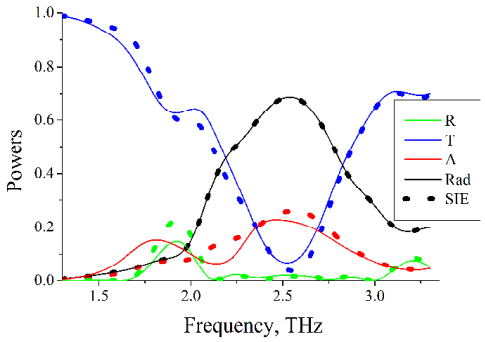

Fig. 2. Dependences of the reflection R, transmission T, absorption A, and radiation Rad coefficients (power) on the frequency, $N = 5$, $\mu_c = 1$ eV. For comparison the results obtained by the method of SIE are shown as dots.

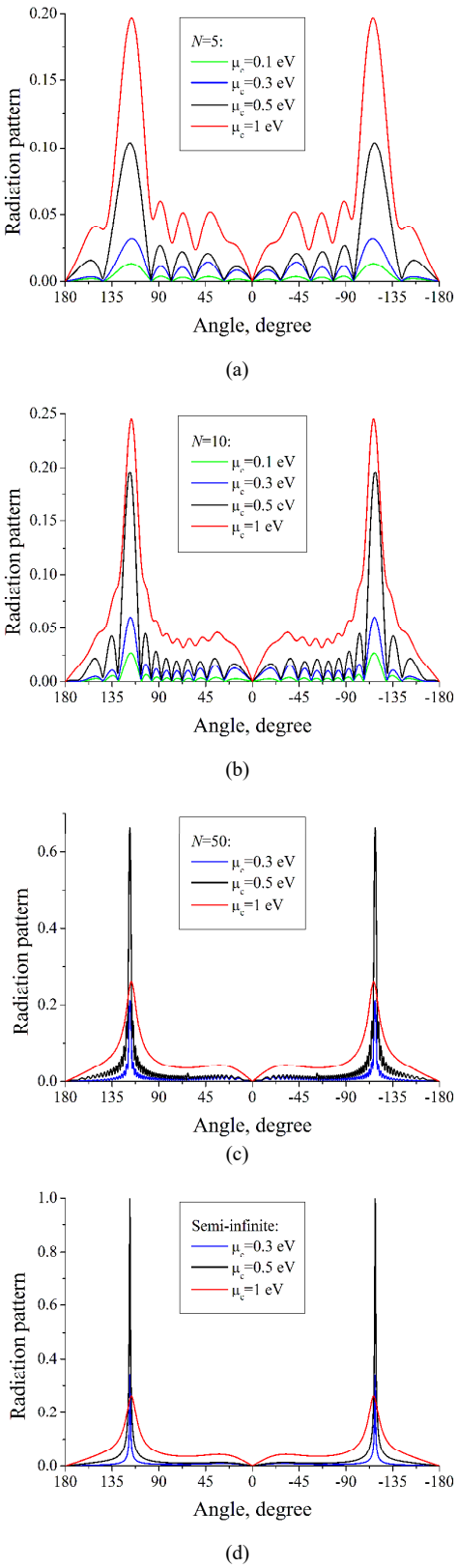

Fig. 3. Normalized radiation patterns, $f = 2.525$ THz. (a) $N = 5$; (b) $N = 10$; (c) $N = 50$; (d) semi-infinite structure.

Fig.3 shows the normalized radiation patterns (amplitude) for the finite and semi-infinite system of strips. With the number of strips is increased, the number of the side-lobes also increases, and their magnitude approaches to the limit case which corresponds to the semi-infinite structure. Graphene conductivity σ has strong dependence on the chemical potential μ_c . This allows to tune the main-lobe level in a large interval.

VI. Conclusion

In this paper, the operator method is used to obtain approximate solution of the dielectric waveguide eigenwaves scattering by finite and semi-infinite system of graphene strips. The maximum of the main lobe level of the radiation pattern can be controlled by variation of the chemical potential. The patterns for the finite structure approach to that of the semi-infinite one with the number of strips is increased.

References

[1] T. Itoh, “Application of Gratings in a Dielectric Waveguide for Leaky-Wave Antennas and Band-Reject Filters (Short Papers),” IEEE Trans. Microwave Theory Techn., vol. 25, no. 12, pp. 1134–1138, Dec. 1977.

[2] M. Tamagnone, J. S. Gómez-Díaz, J. R. Mosig, and J. Perruisseau-Carrier, “Reconfigurable terahertz plasmonic antenna concept using a graphene stack,” Appl. Phys. Lett., vol. 101, no. 21, p. 214102, Nov. 2012.

[3] W. Fuscaldo, P. Burghignoli, P. Baccarelli, and A. Galli, “Efficient 2-D leaky-wave antenna configurations based on graphene metasurfaces,” Int. J. Microw. Wireless Technol., vol. 9, no. 6, pp. 1293–1303, May 2017.

[4] G. W. Hanson, “Dyadic Green“s functions and guided surface waves for a surface conductivity model of graphene,” Journal of Applied Physics, vol. 103, no. 6, p. 064302, Mar. 2008.

[5] R. A. Depine, "Graphene Optics: Electromagnetic Solution of Canonical Problems," IOP Publishing, 2016. doi: 10.1088/978-1-6817-4309-7

[6] N. Xu, J. Chen, J. Wang, X. Qin, and J. Shi, “Dispersion HIE-FDTD method for simulating graphene-based absorber,” IET Microwaves, Antennas & Propagation, vol. 11, no. 1, pp. 92–97, Jan. 2017.

[7] O. V. Shapoval and A. I. Nosich, “Bulk refractive-index sensitivities of the THz-range plasmon resonances on a micro-size graphene strip,” J. Phys. D: Appl. Phys., vol. 49, pp. 055105, 2016.

[8] S. V. Dukhopelnykov, R. Sauleau, and A. I. Nosich, “Integral equation analysis of terahertz backscattering from circular dielectric rod with partial graphene cover,” IEEE J. Quantum Electron., vol. 56, pp. 1–8, 2020.

[9] M. Kaliberda, L. Lytvynenko, and S. Pogarsky, “Singular integral equations in diffraction by multilayer grating of graphene strips in the THz range,” Eur. Phys. J. Appl. Phys., vol.82, pp. 21301, 2018.

[10] L. M. Lytvynenko, I. I. Reznik, D. L. Lytvynenko, “Waves Diffraction on the Semiinfinite Periodical Structures,” Proc. of the Academy of Sciences of the Ukrainian SSR. no. 6, pp.62-66, 1991. (in Russian)

[11] S. N. Vorobyov, and L. M. Lytvynenko, “Electromagnetic wave diffraction by semi-infinite strip grating,” IEEE Trans. Antennas Propag., vol. 59, no. 6, pp. 2169-2177, June 2011.

[12] M. E. Kaliberda and S. A. Pogarsky, “Operator method in a plane waveguide eigenmodes diffraction problem by finite and semiinfinite system of slots,” Int. Conf. on Mathematical Methods in Electromagnetic Theory (MMET), Kharkov, Ukraine, 130-133, 2012.

[13] M. E. Kaliberda, L. M. Lytvynenko, S. A. Pogarsky, “THz waves scattering by finite graphene strip grating embedded into dielectric slab,” IEEE Journal of Quantum Electronics, vol. 56, pp. 8500107, Jan. 2020.

Operator Method in the E-Polarized Plane Wave Scattering by Coplanar Half-Plane and Disk: Basic Equations and Convergence

Mstislav E. Kaliberda
School of Radiophysics, Biomedical Electronics and Computer Systems
V.N. Karazin Kharkiv National University
Kharkiv, Ukraine
KaliberdaME@gmail.com

Sergey A. Pogarsky
School of Radiophysics, Biomedical Electronics and Computer Systems
V. Karazin Kharkiv National University
Kharkiv, Ukraine
Sergey.A.Pogarsky@univer.kharkov.ua

Leonid M. Lytvynenko
Institute of Radio Astronomy of the National Academy of Sciences of Ukraine
Kharkiv, Ukraine
lnl@rian.kharkov.com

***Abstract*— The scattering of the E-polarized wave by the system which consists of a half-plane and a disk is considered. The operator method is used. Basic equations are presented and their discretization is discussed. The numerical convergence is studied.**

Keywords—half-plane, disk, operator method, scattering

I. Introduction

A half-plane and a disk are classical scattering objects. The method due to D. S. Jones, the Wiener-Hopf technique, the method of integral equations, when the scattered field is expressed in terms of the currents on the conductor, the method of dual integral equations, when the scattered field is expressed in terms of Fourier integral of spectral function (Fourier amplitude) are discussed in [1-3] for the half-plane.

The scattering by the disk is considered in [4, 5] with the use of the power series expansion and spheroidal wave function. In [6], the unknown spectral function is expressed in terms of the series of integrals of Bessel functions, which are converted to the hypergeometric polynomial. In [7], the method of dual integral equations is used. The Fredholm integral equations are obtained for the thin disk of finite thickness in [8]. In [9], the authors perform analytical regularization and discretization within one procedure, namely Galerkin projection on the set of judicious expansion functions, which are the eigenfunctions of the singular (static) part.

In this paper, we consider scattering by the structure which consists of the half-plane and circular disk. To solve the problem we use the operator method. The unknown Fourier amplitudes can be found from the operator equations. These equations use the scattering operators of a single discontinuity.

In previous papers, the operator method is successfully applied to the periodic structures with the scattered fields with discrete spectrum (represented as Fourier series) [10, 11] or to the gratings with continuous spatial spectrum (represented as Fourier integrals) [12]. In [13], the semi-infinite strip grating with scattered field, which has both discrete and continuous spectrum is considered. Such field can be represented as a superposition of the plane wave and cylindrical waves.

Here, in this paper, we initiate the study of the structure with the scattered field, which can be represented as a sum of the field of plane, cylindrical and spherical waves.

II. Problem Statement

We consider the perfectly electric conducting half-plane, $-\infty < x < \infty$, $y < 0$, $z = 0$, and the disk with center at the point $x = 0$, $y = \Delta$, $z = 0$ having radius r. Distance between the half-plane and disk is $\Delta - r$. The geometry of the structure is shown in Fig.1. The time dependence is $\exp(-i\omega t)$.

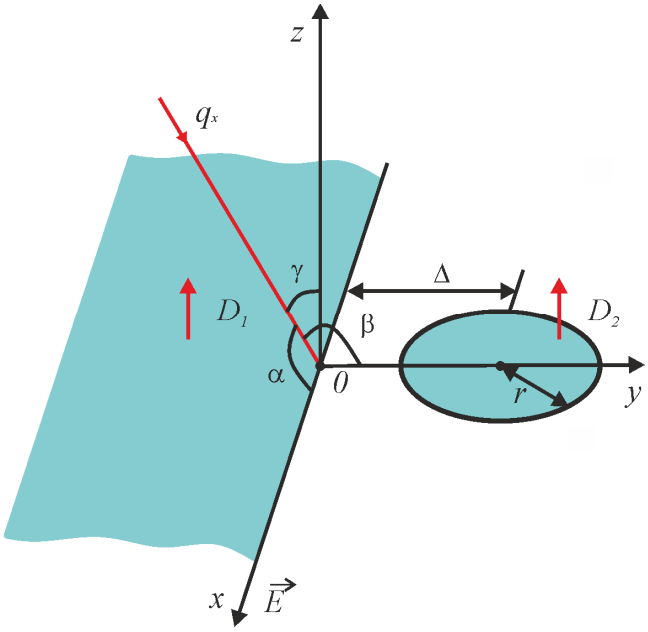

Fig. 1. Structure geometry.

Suppose that E plane wave is incident from the domain $z > 0$. Its tangential electric field components are

$$E_x^i = q_x \exp\left(ik(\alpha x + \beta y - \gamma(\alpha,\beta)z)\right),\ E_y^i = 0, \qquad (1)$$

where k is the wavenumber, α, β are real constants, $\gamma(\alpha,\beta) = \sqrt{1-\alpha^2-\beta^2}$ with $\mathrm{Re}\,\gamma \geq 0$, $\mathrm{Im}\,\gamma \geq 0$, q_x is the amplitude, $q = (q_x, 0)^*$. Values α, β, and $\gamma(\alpha,\beta)$ are cosines of the angles of the wavevector of the incident field relatively to the x, y, and z axis.

978-1-6654-0093-0/21/$31.00 ©2021 IEEE

The electromagnetic field can be expressed in terms of two electric components E_x and E_y. We consider problem in the spectral domain, i.e. in the domain of Fourier transform. The total electromagnetic field we seek as a sum of the incident and scattered field, $E_\Theta = E_\Theta^i + E_\Theta^s$, $\Theta = x, y$. Scattered field, in turn, we seek as a sum of the field scattered by the half-plane with the amplitude $D_1 = (D_{1,x}, D_{1,y})^*$ and by the disk with the amplitude $D_2 = (D_{2,x}, D_{2,y})^*$,

$$E_\Theta^s(x,y,z) = \int_{-\infty}^{\infty}\int_{-\infty}^{\infty}(D_{1,\Theta}(\xi_x,\xi_y) + D_{2,\Theta}(\xi_x,\xi_y)) \times \exp\left(ik(\xi_x x + \xi_y y + \gamma(\xi_x,\xi_y)|z|)\right)d\xi_x d\xi_y. \quad (2)$$

Let us introduce reflection operator of the isolated half-plane R_1 and of the isolated disk R_2 with center at the origin, $x = 0$, $y = 0$, $z = 0$,

$$R_j = \begin{pmatrix} R_{j,xx} & R_{j,xy} \\ R_{j,yx} & R_{j,yy} \end{pmatrix},\ j = 1,2, \quad (3)$$

by the formula

$$C_{j,\Theta}(\xi_y,\xi_y) = \sum_{\Xi=x,y}\int_{-\infty}^{\infty}\int_{-\infty}^{\infty}R_{j,\Theta,\Xi}(\xi_x,\xi_y,\zeta_x,\zeta_y) \times g_\Xi(\zeta_x,\zeta_y)d\zeta_x d\zeta_y,\ \Theta = x,y, \quad (4)$$

where $C_j = (C_{j,x}, C_{j,y})^*$ is the Fourier amplitude of the field reflected by the isolated half-plane, $j = 1$, or by the isolated disk, $j = 2$, $g = (g_x, g_y)^*$ is the Fourier amplitude of the incident field. Operator R_1 can be found by the factorization method [3], and operator R_2 can be found by the method described in [6].

III. Solution of the Problem

A. Operator equations

The operator equations relatively unknown Fourier amplitudes of the scattered field are

$$D_1 = R_1 D_2 + R_1 q, \quad (5)$$

$$D_2 = S^- R_2 S^+ D_1 + S^- R_2 S^+ q, \quad (6)$$

where operators $S^\pm$ define the phase variation when the coordinate system is shifted in the positive (negative) direction of the y - axis.

The explicit form of the operator R_2 is known and not shown here, however we need to discuss the behavior of its kernel-function near the singular points. The kernel function of the operator R_2 can be represented as

$$R_{2,\Theta,\Xi}(\xi_x,\xi_y) = R_{\Theta,\Xi}(\xi_x,\xi_y)/\sqrt{1-\xi_x^2-\xi_y^2}, \quad (7)$$

where $R_{\Theta,\Xi}(\xi_x,\xi_y)$ has already no singularities, $\Theta = x, y$, $\Xi = x, y$.

After substitution of the explicit expression of the operator R_1 into (5), and (7) into (6), taking into account (4), we can rewrite operator equations (5), (6) in the form of the integral equations.

Since kernel-functions of the operators R_1 and R_2 have singularities, unknown Fourier amplitudes D_1, D_2 also can have singularities at the same points. Let us introduce new regular functions.

$$F_{1,x}(\xi_x,\xi_y) = \left(D_{1,x}(\xi_x,\xi_y) + \frac{i}{2\pi}\frac{\sqrt{\sqrt{1-\alpha^2}-\beta}}{\sqrt{\sqrt{1-\alpha^2}-\xi_y}}\frac{q_x}{\xi_y - \underset{below}{\beta}}\right)\sqrt{1-\xi_x^2-\xi_y^2}, \quad (8)$$

$$F_{1,y}(\xi_x,\xi_y) = \sqrt{1-\xi_x^2-\xi_y^2}\left(D_{1,y}(\xi_x,\xi_y) + \frac{i}{2\pi}\frac{\alpha}{\sqrt{1-\alpha^2}}\frac{q_x}{\sqrt{\sqrt{1-\alpha^2}-\beta}\sqrt{\sqrt{1-\alpha^2}-\xi_y}}\right), \quad (9)$$

$$F_{2,\Theta}(\xi_x\xi_y) = D_{2,\Theta}(\xi_x,\xi_y)\sqrt{1-\xi_x^2-\xi_y^2}, \quad (10)$$

Taking into account that we consider only the E - polarized incident field, substituting (8)-(10) as well as the explicit expression of the operator R_1 into (5), (6), one can finally obtain the following integral equations relatively regular function $F_{j,\Theta}(\xi_x,\xi_y)$:

$$F_{1,x}(\xi_x,\xi_y) = \frac{i}{2\pi}\sqrt{\sqrt{1-\xi_x^2}+\xi_y} \times \int_{-\infty}^{\infty}\frac{F_{2,x}(\xi_x,\zeta_y)}{\sqrt{\sqrt{1-\xi_x^2}+\zeta_y}}\frac{d\zeta_y}{\zeta_y - \underset{below}{\xi_y}}, \quad (11)$$

$$F_{1,y}(\xi_x,\xi_y) = \frac{i}{2\pi}\sqrt{\sqrt{1-\xi_x^2}+\xi_y} \times \int_{-\infty}^{\infty}\frac{F_{2,x}(\xi_x,\zeta_y)}{\sqrt{1-\xi_x^2-\zeta_y^2}}\frac{\xi_x}{\sqrt{1-\xi_x^2}}\frac{d\zeta_y}{\sqrt{\sqrt{1-\xi_x^2}-\zeta_y}} + \frac{i}{2\pi}\sqrt{1-\xi_x^2-\xi_y^2} \times \int\frac{\sqrt{\sqrt{1-\xi_x^2}-\xi_y}}{\sqrt{\sqrt{1-\xi_x^2}-\zeta_y}}\frac{F_{2,y}(\xi_x,\zeta_y)}{\sqrt{1-\xi_x^2-\zeta_y^2}}\frac{d\zeta_y}{\zeta_y - \underset{below}{\xi_y}}, \quad (12)$$

$$F_{2,\Theta}(\xi_x,\xi_y)\exp(ik\xi_y\Delta)=\sum_{\Xi=x,y}\int_{-\infty}^{\infty}\frac{\exp(ik\zeta_y\Delta)}{\sqrt{1-\zeta_x^2-\zeta_y^2}}\times F_{1,\Xi}(\zeta_x,\zeta_y)R_{\Theta,\Xi}(\xi_x,\xi_y,\zeta_x,\zeta_y)d\zeta_x d\zeta_y$$
$$-\frac{iq_x}{2\pi}\sqrt{\sqrt{1-\alpha^2}-\beta}\int_{-\infty}^{\infty}\frac{\exp(ik\zeta_y\Delta)R_{\Theta,x}(\xi_x,\xi_y,\alpha,\zeta_y)}{\sqrt{\sqrt{1-\alpha^2}-\zeta_y}}\times\frac{d\zeta_y}{\zeta_y-\underset{above}{\beta}}+\frac{iq_x}{2\pi}\frac{\alpha}{\sqrt{1-\alpha^2}}\frac{1}{\sqrt{\sqrt{1-\alpha^2}-\beta}}$$
$$\times\int_{-\infty}^{\infty}\frac{\exp(ik\zeta_y\Delta)R_{\Theta,y}(\xi_x,\xi_y,\alpha,\zeta_y)d\zeta_y}{\sqrt{\sqrt{1-\alpha^2}-\zeta_y}}+\exp(ik\beta\Delta)q_xR_{\Theta,x}(\xi_x,\xi_y,\alpha,\beta). \tag{13}$$

Integrands in (8), (11)-(13) contain non-integrable in general sense singularities of the form $1/x$, if $x\to 0$. To exclude the singularities, the regularization procedure is needed. The purpose of the regularization procedure is to obtain the integrals with the regular or integrable integrands to which the general methods of numerical integration can be applied.

B. Regularization

The ideas of the regularization procedure are as follows. Taking into account the radiation conditions, we transform the integration path $-\infty<\xi<\infty$ in the complex plane so that it bypasses singularities from above or below (subscript "above" or below in (8), (11), (12)). After that, taking into account that $\int_{-\infty}^{\infty}\frac{d\xi}{\xi-\underset{below}{\zeta}}=\pi i$, $\int_{-\infty}^{\infty}\frac{d\xi}{\xi-\underset{above}{\zeta}}=-\pi i$ we can obtain Cauchy principal value integrals. For example, for the integral $\int_{-\infty}^{\infty}\frac{f(\xi)d\xi}{\xi-\underset{below}{\zeta}}$ the regularization procedure gives:

$$\int_{-\infty}^{\infty}\frac{f(\xi)d\xi}{\xi-\underset{below}{\zeta}}=v.p.\int_{-\infty}^{\infty}\frac{f(\xi)d\xi}{\xi-\zeta}+\pi i f(\zeta), \tag{14}$$

where $f(\xi)$ is an arbitrary non-ascending continuous function such that integral $v.p.\int_{-\infty}^{\infty}\frac{f(\xi)d\xi}{\xi-\zeta}$ is convergent.

After the regularization procedure obtained equations can be solved numerically.

C. Discretization

To discretize the obtained equations we exchange the infinite interval of integration by the symmetric bounded one, $(-a,a)$. Then we divide interval $(-a,a)$ into N equal sub-intervals S_n, $n=0,...,N-1$, where N is odd. On every n th sub-interval $S_n=(-a+2an/N;-a+2a(n+1)/N)$ we take single node point $\eta_n=-a+2a(n+1/2)/N$ and exchange unknown function by the constant:

$$v.p.\int_{-\infty}^{\infty}\frac{f(\xi)h(\xi)d\xi}{\xi-\zeta}\approx v.p.\int_{-a}^{a}\frac{f(\xi)h(\xi)d\xi}{\xi-\zeta}=\sum_{n=0}^{N-1}v.p.\int_{S_n}\frac{f(\xi)h(\xi)d\xi}{\xi-\zeta}\approx\sum_{n=0}^{N-1}f(\eta_n)c_n, \tag{15}$$

where $c_n=v.p.\int_{S_n}\frac{f(\xi)h(\xi)d\xi}{\xi-\zeta}$ are coefficients, $f(\xi)$ is one of the unknown amplitudes, $h(\xi)$ is the weighting function.

Integral of the form $v.p.\int_{S_n}\frac{d\xi}{\xi-\zeta}=\ln\left|\frac{-a+2a(n+1)/N-\zeta}{-a+2an/N-\zeta}\right|$. Integrals of the form $v.p.\int_{S_n}\frac{d\xi}{\xi-\zeta}\frac{1}{\sqrt{A-\xi}}$, $v.p.\int_{S_n}\frac{d\xi}{\xi-\zeta}\frac{1}{\sqrt{A-\xi^2}}$ (A is an arbitrary constant) also can be calculated analytically. However their expressions are too lengthy and are not shown here.

After applying (15) to all integrals in (11)-(13) one can obtain set of linear equations relatively values of the unknown amplitudes at the nodes η_n, $n=0,...,N-1$. This set of equations in the brief form can be written as

$$\hat{F}=\hat{R}\hat{F}, \tag{16}$$

where $\hat{F}$ is the vector of the values of the unknown amplitudes at the nodes, $\hat{R}$ is the matrix obtained after discretization.

To solve (16) we used the iterative procedure, $\hat{F}^{(l)}=\hat{R}\hat{F}^{(l-1)}$, $l=1, 2, 3,...L$, where $\hat{F}^{(l)}$ is the solution obtained at the l th step, L is the total number of iterations. As the initial iteration we take the zero vector, $\hat{F}^{(0)}=0$.

IV. Numerical Results

Let us study the numerical convergence. The error of the results depends on the size of the segment a, number of nodes N and number of iterations L. We introduce relative error as follows:

$$\varepsilon(N)=|D(N)-D(2N-1)|/|D(2N-1)|, \tag{17}$$

$$\delta(L)=|D(L)-D(L+1)|/|D(L+1)|, \tag{18}$$

where $D=\int_{-1}^{1}\left(|D_x(0,\xi_y)|^2+|D_y(0,\xi_y)|^2\right)d\xi_y$ has sense of the power of the scattered spherical waves along the semicircle $\varphi=0^0$ (φ is counted from the x -axis).

Fig.2 shows dependences of the error $\varepsilon(N)$ on the number of nodes, and Fig.3 shows dependences of the error $\delta(L)$ on the number of iteration. Starting from a certain value, the convergence is monotone. With the size of the disk is increased we should take more nodes.

Fig. 4 shows the total field distribution in the plane $x = 0$. The field scattered by the structure consists of three types of waves. Plane wave, which is reflected by the infinite half-plane. Spherical wave, which is scattered by the disk. Cylindrical wave, which is scattered by the end of the half-plane. Reflected plane wave exists only in the domain $y < 0$. Line $y = 0$ acts as a shadow boundary or transition region. The field of the plane wave in the domain $y < 0$ and the field of the combined spherical and cylindrical waves are clearly seen in Fig.4.

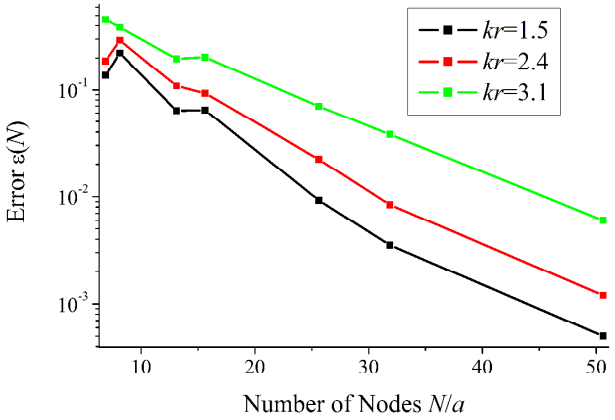

Fig. 2. Error $\varepsilon(N)$ vs. the number of nodes N/a for $\Delta/r = 2$.

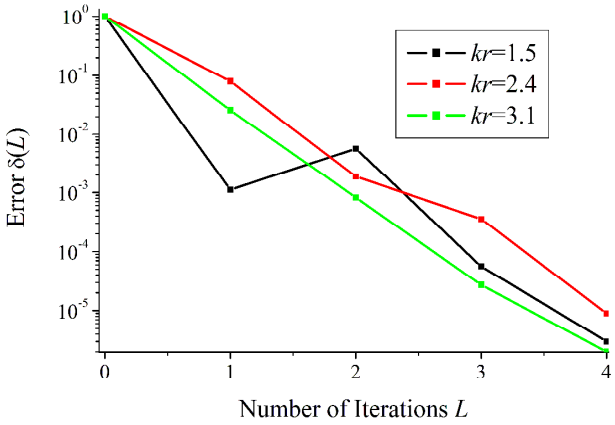

Fig. 3. Error $\delta(L)$ vs. the number of iterations for $\Delta/r = 2$.

V. Conclusion

In this paper, for the first time we initiated the study of the electromagnetic wave scattering by the half-plane and the disk with the use of the operator method. The obtained solution is rigorous. The dependences of an error on the number of nodes and number of iterations are presented. The discretization scheme shows monotone convergence.

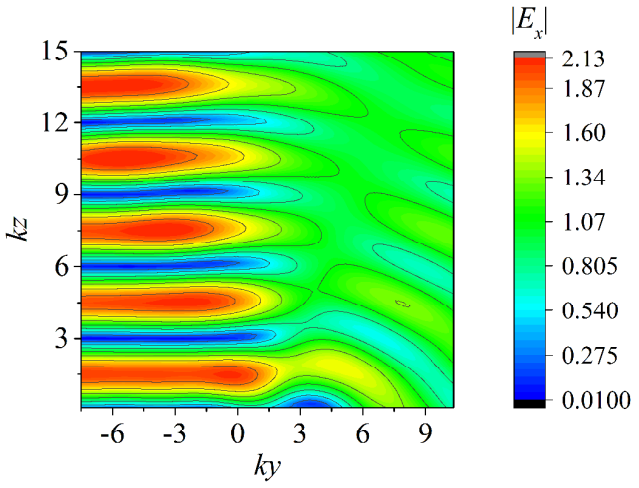

Fig. 4. Total field distribution, $|E_x|$ component, $kr = 1.5$, $\Delta/r = 2$, $kx = 0$.

References

[1] D. S. Jones, "Note on diffraction by an edge," Quart. Journ. Mech. and Applied Math., Vol. 3, no. 4, pp. 420-434, 1950.

[2] D. S. Jones, "A simplifying technique in the solution of a class of diffraction problems," Quart. J. Math. Vol.3, no.1, pp. 189-196, 1952.

[3] D. Noble, "Methods based on the wiener-hopf technique for the solution of partial differential equations," London a.o., Pergamon Press, 1958.

[4] C.J. Bouwkamp, "On the diffraction of electromagnetic waves by small circular disks and holes," Philips Research Reports, vol.5, pp.401-422, 1950.

[5] J. Maixner and W. Andrejewski, "Strenge Theorie der Beugung ebener elektromagnetischer Wellen an der vollkommen leitenden Kreisscheibe und an der kreisförmigen Öffnung im vollkommen leitenden ebenen Schirm," Ann. d. Phys., vol. 442, pp.157-168, 1950.

[6] Y. Nomura and S. Katsura, "Diffraction of electromagnetic waves by circular plate and circular hole," J. Phys. Soc. Jpn., vol. 10, pp. 285-304, 1955.

[7] K. Hongo and Q. A. Naqvi, "Diffraction of electromagnetic wave by disk and circular hole in a perfectly conducting plane," PIER, vol. 68, pp. 113–150, 2007.

[8] M. V. Balaban, R. Sauleau, T. M. Benson, and A. I. Nosich, "Dual integral equations technique in electromagnetic wave scattering by a thin disk," PIER B, vol. 16, pp. 107-126, 2009.

[9] M. Lucido, G. Panariello, and F. Schettino, "Scattering by a zero-thickness PEC disk: A new analytically regularizing procedure based on Helmholtz decomposition and Galerkin method," Radio Sci., vol.52, pp.2-14.

[10] L. M. Lytvynenko, I. I. Reznik, D. L. Lytvynenko, "Waves Diffraction on the Semiinfinite Periodical Structures," Proc. of the Academy of Sciences of the Ukrainian SSR, no. 6, pp.62-66, 1991.

[11] Kaliberda M. E., Litvinenko L. N. and Pogarsky S. A. 2010, "Diffraction of H_{0m} and E_{0m} Modes by a System of Axially Symmetric Discontinuities in a Coaxial Circuit," J. of Commun. Technol. Electron, 2010, vol. 55, no. 5, 505-511.

[12] M. E. Kaliberda, L. M. Lytvynenko, S. A. Pogarsky, and M. P. Roiuk, "Diffraction of the H-polarized plane wave by a finite layered graphene strip grating," Int. J. Microw. Wireless Technol., vol. 11, no. 4, pp. 326-333, Sep. 2018

[13] M. E. Kaliberda, L. M. Lytvynenko, S. A. Pogarsky, "Diffraction of H-polarized electromagnetic waves by a multi-element planar semi-infinite grating," Telecommunications and Radio Engineering, vol. 74, no. 9, pp. 348-357, 2015.